

Image Assimilation and Motion Estimation of Geophysical Fluids

Isabelle Herlin ^a, Dominique Béréziat ^b Étienne Huot ^c

^aINRIA, France.

CEREA, joint laboratory ENPC-EDF R&D, Université Paris-Est, France.
(Isabelle.Herlin@inria.fr)

^bUniversité Pierre et Marie Curie, Paris, France (Dominique.Bereziat@upmc.fr)

^cUniversité Versailles Saint-Quentin en Yvelines, France (Etienne.Huot@inria.fr)

Abstract Simulation models and image data are simultaneously available for numerous scientific domains, such as oceanography and meteorology. They are indeed two complementary descriptions of the same complex system. Data Assimilation is a well-known mathematical technique used, in environmental sciences, to improve forecasts obtained from the simulation models, thanks to the observation data. One class of data assimilation algorithms, named 4D-Var, globally adjusts the model output to the observations, that are available over a period of time. The question of how to derive accurate characteristic features from images, with an optimal use of the simulation model, is of major interest for the image processing community. In this article, we consider applying data assimilation methods for motion estimation on a sequence of satellite images acquired over the ocean. We describe various strategies that can be derived in the framework of variational data assimilation (4D-Var). They mostly depend on the choice of the state vector itself. According to this definition, the dynamics has to be described and observation operators specified in order to characterize the information displayed by the image sequence. We detail the mathematical setting of these strategies and analyze their properties. Results are provided on twin experiments to quantify the methods and on satellite acquisitions acquired over the Black Sea.

Keywords: Data Assimilation; Motion; Satellite Images

1 INTRODUCTION

Simulation models and image data are simultaneously available for numerous scientific domains such as oceanography, meteorology, hydrology, glaciology, atmosphere chemistry, engineering, biology, and medicine. In all cases, complex numerical models have been settled, and huge amounts of different kinds of data, including image acquisitions, provide a deep insight on the observed phenomenon. Models and images are indeed two complementary descriptions of the same reality. Two questions arise from that remark. From the model viewpoint: how to improve the forecasts obtained by a simulation model with a better use of the image information? From the image viewpoint: how to derive accurate characteristic features from images by making an optimal use of these models? The paper focuses on this last question and describes the available options to be settled in order to define the best strategy for image assimilation according to the applicative context. The discussion is illustrated on the geophysical fluid flow motion estimation issue. Reader is referred to Ruhnau et al. [2007] for a short survey of fluid flow motion estimation methods.

Let $\mathbf{x} = (x, y)$ denote the spatial location on 2D image data and t denote time. As explained in Béréziat and Herlin [2011], an ill-posed image processing problem, such as estimating the motion field $\mathbf{W}(\mathbf{x}, t)$ from an image sequence $I(\mathbf{x}, t)$, is successfully solved in the data assimilation framework if the following information is available:

- a dynamic model, also named evolution equation, for $\mathbf{W}(\mathbf{x}, t)$,
- an equation linking $\mathbf{W}(\mathbf{x}, t)$ and the image data $I(\mathbf{x}, t)$, even in an implicit way: $\mathbb{I}(\mathbf{W}(\mathbf{x}, t), I(\mathbf{x}, t)) = 0$.

Several data assimilation systems can be derived from these two equations. They correspond to various definitions of the state vector and observation operator. Each formulation is a strategy for combining images and model, whose performances depend on the studied problem and on image properties.

The article is organized as follows. Section 2 briefly presents the variational data assimilation concepts. Section 3 discusses the pros and cons of involving pseudo-images in the state vector. Illustration is given in Section 4 on the issue of motion estimation from an image sequence. Observation operators are described in the same section. Experimental results are discussed in Section 5. Section 6 ends the paper with some conclusions and perspectives on the image assimilation issue.

2 VARIATIONAL DATA ASSIMILATION

Let us first summarize the major principles of variational data assimilation.

2.1 Equations of the data assimilation system

Let \mathbf{X} being a state vector depending on the spatial location \mathbf{x} and time t . \mathbf{X} is defined on $A = \Omega \times [t_0, t_1]$, Ω being the bounded spatial domain and $[t_0, t_1]$ the temporal domain. We assume that \mathbf{X} is evolving in time according to:

$$\frac{\partial \mathbf{X}}{\partial t}(\mathbf{x}, t) + \mathbb{M}(\mathbf{X})(\mathbf{x}, t) = 0 \quad (1)$$

\mathbb{M} is the *evolution model*, supposed differentiable. This model is derived from the physical equations that describe the studied system.

Observation images $I(\mathbf{x}, t)$ are available. They are linked to the state vector through an observation equation:

$$\mathbb{H}(\mathbf{X}, I)(\mathbf{x}, t) = 0 \quad (2)$$

\mathbb{H} is the *observation operator*, supposed differentiable.

We consider having some knowledge on the initial condition of the state vector at $t = t_0$. This is the *background* value $\mathbf{X}_b(\mathbf{x})$, that is given as initial condition of the state vector at the beginning of the assimilation process:

$$\mathbf{X}(\mathbf{x}, t_0) - \mathbf{X}_b(\mathbf{x}) = 0 \quad (3)$$

2.2 Variational formulation

In order to solve System (1,2,3), the following functional is defined and has to be minimized:

$$\begin{aligned}
 E(\mathbf{X}) = & \frac{1}{2} \int_A \int_A \left(\frac{\partial \mathbf{X}}{\partial t} + \mathbb{M}(\mathbf{X}) \right)^T (\mathbf{x}, t) Q^{-1} \left(\frac{\partial \mathbf{X}}{\partial t} + \mathbb{M}(\mathbf{X}) \right) (\mathbf{x}', t') dx dt dx' dt' \\
 & + \frac{1}{2} \int_A \int_A \mathbb{H}(\mathbf{X}, \mathbf{Y})^T (\mathbf{x}, t) R^{-1} (\mathbf{x}, t, \mathbf{x}', t') \mathbb{H}(\mathbf{X}, \mathbf{Y}) (\mathbf{x}', t') dx dt dx' dt' \quad (4) \\
 & + \frac{1}{2} \int_{\Omega} \int_{\Omega} (\mathbf{X}(\mathbf{x}, t_0) - \mathbf{X}_b(\mathbf{x}))^T B^{-1} (\mathbf{x}, \mathbf{x}') (\mathbf{X}(\mathbf{x}', t_0) - \mathbf{X}_b(\mathbf{x}')) dx dx'
 \end{aligned}$$

$E(\mathbf{X})$ expresses that each one of Equations (1) to (3) is not exactly verified: the right terms are not null and usually modeled by Gaussian error variables, Tarantola [2005]. Q , R and B represent their respective covariance matrices. The first term of $E(\mathbf{X})$ means that even the evolution equation is not exactly verified: the model is said imperfect, Tremolet [2006]. Minimization of E is carried out with an incremental method, that is extensively described in Béréziat and Herlin [2011].

3 DEFINITION OF \mathbf{X} . WITH OR WITHOUT PSEUDO-IMAGES?

One core discussion of the paper concerns the involvement of pseudo-images in the state vector. Let first define some notations. Consider that our problem is to estimate a quantity \mathbf{Z} from an image sequence I and is described by the following mathematical relation between I and \mathbf{Z} :

$$\mathbb{I}(\mathbf{Z}, I)(\mathbf{x}, t) = 0 \quad (5)$$

at each space-time location. This is an implicit formulation of image processing problems, such as, for instance, optical flow estimation, curves matching and tracking of objects. When applying image assimilation methods, the first issues to be considered are the definition of the state vector \mathbf{X} and of its evolution model \mathbb{M} .

Two main options are available at first look.

First, the state vector, denoted \mathbf{X}_1 , is equal to the studied quantity \mathbf{Z} and the model \mathbb{M}_1 describes its dynamics. The observation vector \mathbf{Y}_1 is the sequence of images, I , and the inverse problem equation (5) is chosen as observation equation (2). This is the *direct assimilation of images*, described by the system:

$$\begin{aligned}
 \mathbf{X}_1(\mathbf{x}, t) &= \mathbf{Z}(\mathbf{x}, t) \\
 \mathbf{Y}_1 &= I \\
 \mathbb{H}_1(\mathbf{X}_1, \mathbf{Y}_1) &= \mathbb{I}(\mathbf{Z}, I)
 \end{aligned} \quad (6)$$

Discussions on the operator \mathbb{H}_1 is given in Section 4 in case of motion estimation.

Second, the state vector, denoted \mathbf{X}_2 , includes an additional component $I_s(\mathbf{x}, t)$, named pseudo-image, that is similar to the observed images and evolves in time according to the same heuristics. The observation vector \mathbf{Y} is again the sequence of observed images I . However, the comparison of the state vector with the image observations becomes the difference of the pseudo-image with the real one at acquisition dates. The corresponding assimilation system is:

$$\begin{aligned}
 \mathbf{X}_2(\mathbf{x}, t) &= (\mathbf{Z}(\mathbf{x}, t) \quad I_s(\mathbf{x}, t))^T \\
 \mathbf{Y}_2 &= I \\
 \mathbb{H}_2(\mathbf{X}_2, \mathbf{Y}_2) &= \mathbb{P}_s(\mathbf{X}_2) - \mathbf{Y}_2 = I_s - I
 \end{aligned} \quad (7)$$

with T the transpose operator and \mathbb{P}_s the projection on the I_s -component. This is named *pseudo-image approach*.

Having involved a pseudo-image in the state vector, a number of new strategies are now available to the user. The question is: is it better to assimilate the image data I or to assimilate pseudo-observations derived from them? In that last case, a transform \mathcal{T} is first applied to the observe images and a new data assimilation system is obtained:

$$\begin{aligned} \mathbf{X}_3(\mathbf{x}, t) &= (\mathbf{Z}(\mathbf{x}, t) \quad I_s(\mathbf{x}, t))^T \\ \mathbf{Y}_3 &= \mathcal{T}(I) \\ \mathbb{H}_3(\mathbf{X}_3, \mathbf{Y}_3) &= d(\mathcal{T}(\mathbb{P}_s(\mathbf{X}_3)), \mathbf{Y}_3) = d(\mathcal{T}(I_s), \mathcal{T}(I)) \end{aligned} \quad (8)$$

d being a measure of the discrepancy between the transform of I_s and that of I in the space of transform coefficients. This is, for instance, applied by Titaud et al. [2010], with \mathcal{T} being the curvelet transform. In the general case, \mathcal{T} is used to quantify major characteristics of the image data and to filter noise that occurred during the acquisition, in order to improve the retrieval of \mathbf{Z} from the images I . The data that are assimilated in the model are no more the raw observations, but pseudo-observations computed by the numerical process associated with \mathcal{T} . In this case, performances of \mathcal{T} strongly impact the results. This is named *pseudo-image approach with assimilation of pseudo-observations*. Reader should refer to Titaud et al. [2010] for a full description of the method, that is no more discussed in the following.

The *pseudo-image approach* is attractive, due to the simple observation operator involved in System (7). An evolution equation of I_s is however required, based on the knowledge on the evolution of image acquisitions:

$$\frac{\partial I_s}{\partial t}(\mathbf{x}, t) + \mathbb{F}(I_s)(\mathbf{x}, t) = 0 \quad (9)$$

The evolution model of \mathbf{X}_2 is equal to $(\mathbb{M}_1 \quad \mathbb{F})^T$, \mathbb{M}_1 being the dynamic model of \mathbf{Z} . \mathbb{F} is often chosen as the transport equation, as described in Horn and Schunk [1981]:

$$\frac{\partial I_s}{\partial t}(\mathbf{x}, t) + \nabla I_s(\mathbf{x}, t) \cdot \mathbf{W}(\mathbf{x}, t) = 0 \quad (10)$$

with $\mathbf{W}(\mathbf{x}, t)$ being the motion field on the space-time domain, $\nabla I_s(\mathbf{x}, t)$ being the spatial gradient of I_s , and \cdot denoting the dot product.

4 MOTION ESTIMATION ISSUE

In this section, the *direct assimilation of images* and the *pseudo-image approach* are discussed for the motion estimation issue. The problem is to retrieve the motion field $\mathbf{W}(\mathbf{x}, t)$ from an image sequence $I(\mathbf{x}, t)$, assuming that grey level values are advected by the motion field:

$$\mathbb{I}(\mathbf{W}, I)(\mathbf{x}, t) = \frac{\partial I}{\partial t}(\mathbf{x}, t) + \nabla I(\mathbf{x}, t) \cdot \mathbf{W}(\mathbf{x}, t) = 0 \quad (11)$$

Direct assimilation of images is first implemented. By identifying with System (6), we get:

$$\begin{aligned} \mathbf{X}_1(\mathbf{x}, t) &= \mathbf{W}(\mathbf{x}, t) \\ \mathbf{Y}_1(\mathbf{x}, t) &= I(\mathbf{x}, t) \\ \mathbb{H}_1(\mathbf{X}_1, \mathbf{Y}_1)(\mathbf{x}, t) &= \frac{\partial I}{\partial t}(\mathbf{x}, t) + \nabla I(\mathbf{x}, t) \cdot \mathbf{W}(\mathbf{x}, t) \end{aligned}$$

The Lagrangian constancy of velocity, $\frac{d\mathbf{W}}{dt} = 0$, is taken as dynamic model \mathbb{M}_1 of \mathbf{W} :

$$\frac{d\mathbf{W}}{dt} = \frac{\partial\mathbf{W}}{\partial t} + (\mathbf{W} \cdot \nabla)\mathbf{W} = 0 \quad (12)$$

Applying the *direct assimilation* approach requires first having processed the image sequence and computed the space and time gradients used in the observation equation. This makes the process highly dependent on the quality of this preprocessing. Moreover, Eq. (11) assumes that motion is constant over the time interval used for computing the temporal gradient $\frac{\partial I}{\partial t}(\mathbf{x}, t)$. This is incoherent with using a dynamic model \mathbb{M}_1 for \mathbf{W} . This inconsistency in the data assimilation system has a negative impact on results as it will be shown in the next section. Last, Eq. (11) is a linearized version of the brightness transport equation, and is only valid if the time interval between two observation images is small enough. If not, Eq. (11) is no more correctly handling the dynamics visualized by the image sequence: displacements between frames are too large to be modeled by that equation.

In the *pseudo-image approach*, we identify with System (7) and get:

$$\begin{aligned} \mathbf{X}_2(\mathbf{x}, t) &= (\mathbf{W}(\mathbf{x}, t) \quad I_s(\mathbf{x}, t))^T \\ \mathbf{Y}_2(\mathbf{x}, t) &= I(\mathbf{x}, t) \\ \mathbb{H}_2(\mathbf{X}_2, \mathbf{Y}_2)(\mathbf{x}, t) &= I_s(\mathbf{x}, t) - I(\mathbf{x}, t) \end{aligned}$$

The pseudo-image I_s has the same dynamics than the observations I : advection of grey level values by the motion field. As the time step dt of the simulation process is controlled by the user, the equation remains valid during the temporal integration, even if the time interval between image acquisitions is large. The evolution of \mathbf{X}_2 is described by:

$$\frac{\partial\mathbf{W}}{\partial t} + (\mathbf{W} \cdot \nabla)\mathbf{W} = 0 \quad (13)$$

$$\frac{\partial I_s}{\partial t} + \mathbf{W} \cdot \nabla I_s = 0 \quad (14)$$

and the evolution model is:

$$\begin{aligned} \mathbb{M}_2(\mathbf{X}_2) &= (\mathbb{M}_1(\mathbf{X}_2) \quad \mathbb{F}(\mathbf{X}_2))^T \\ &= ((\mathbf{W} \cdot \nabla)\mathbf{W} \quad \mathbf{W} \cdot \nabla I_s)^T \end{aligned}$$

5 RESULTS

5.1 Twin experiments

The *direct assimilation of images* is compared to the *pseudo-image approach* on twin experiments in order to quantify differences. A synthetic image sequence is obtained from the initial conditions, displayed in Figure 1, using the transport of brightness and Lagrangian constancy of motion equations. Six images of that simulation are used as observations for image assimilation and displayed on Figure 2.

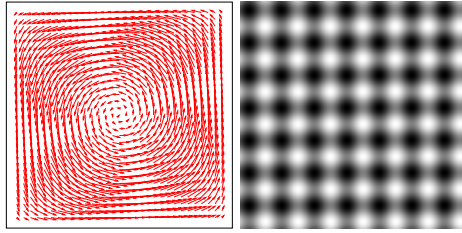


Figure 1. Left: initial motion field. Right: initial value of I_s .

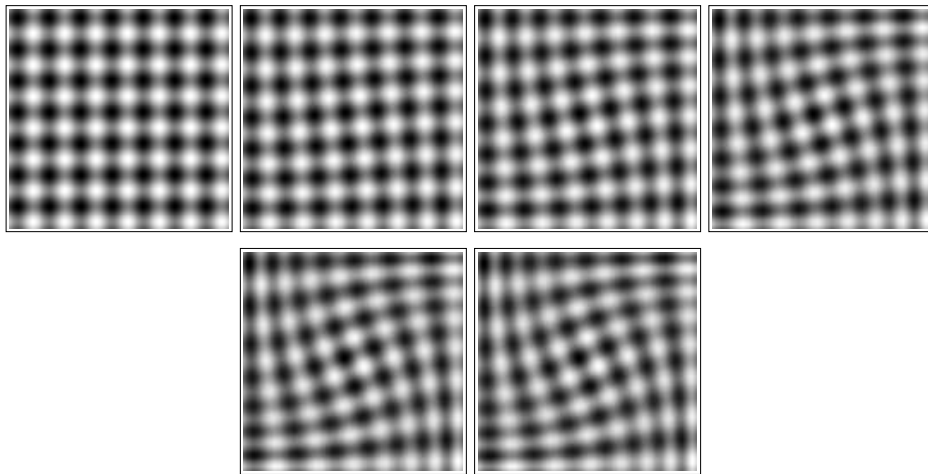


Figure 2. Observations.

The *direct assimilation of images* is named IME (Image Model External) as the images are External to the state vector, while the *pseudo-image approach* is named IMI (Image Model Included) as pseudo-images I_s are Included in the state vector. The same observations are used for both assimilations. Results are displayed on Figure 3 and compared to the effective motion field. Statistics are given in Table 1. The first column is the average of the relative error of the euclidian norm. The second column is the average of the absolute value of orientation error. Better results are obtained with IMI, due to its improved comparison of the state vector with the observations. The advantage of IMI is even more visible if the time interval between observation increases.

5.2 Satellite data

Image assimilation is then applied to retrieve surface currents on Sea Surface Temperature data (SST). The satellite images have been acquired by NOAA-AVHRR sensors, over the Black Sea, and displayed on Fig. 4. The two image assimilation methods are

Table 1. Error statistics.

	Norm (%)	Orientation (in degree)
IME	27.9	2.128
IMI	9.8	0.792

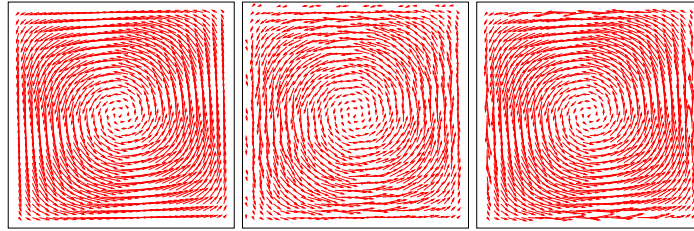


Figure 3. Left: Ground truth. Center: IME. Right: IMI.

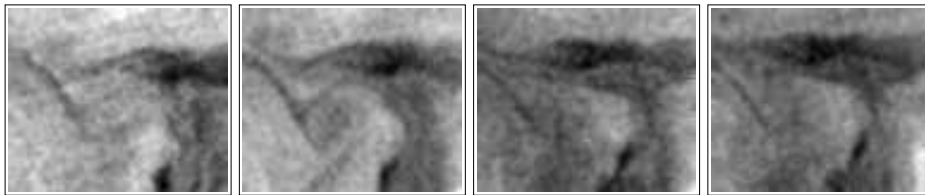


Figure 4. Satellite observations.

used and the estimated motion fields are given on Fig. 5. Only qualitative comparison is at hand, as no ground truth is available in that case. For instance, the counter-clockwise rotational motion occurring in the bottom-left part of the image sequence is correctly retrieved by IMI and missed by IME.

6 CONCLUSION

The paper describes issues that have to be considered, when applying image assimilation to solve an image processing problem.

The first option is to decide including or not pseudo-images in the state vector: *direct assimilation of images* or *pseudo-image approach*. These pseudo-images allow an easy comparison with the image observations. However, they increase the memory required for the assimilation process. Moreover, their dynamics has to be correctly handled. Otherwise, the comparison with image observations is no more significant. If the transport equation is valid, then the *pseudo-image approach* is the most advantageous, compared to the *direct assimilation of images*. Indeed, it successfully processes sequences of images with large time interval between frames, if the user chooses the correct time interval dt of the simulation. In the paper, experiments have been described for motion estimation on synthetic and real data. They proved the improvements that can be obtained with the *pseudo-image approach*.

Perspectives of the work will first be to compare various dynamic equations of \mathbf{W} for *direct assimilation of images* and *pseudo-image approach*. In a second phase, these two approaches will be compared on a new image processing issue such as curve tracking.

ACKNOWLEDGEMENTS

Satellite data have been provided by E. Plotnikov and G. Korotaev from the Marine Hydrophysical Institute of Sevastopol, Ukraine. Research has been partly funded by the

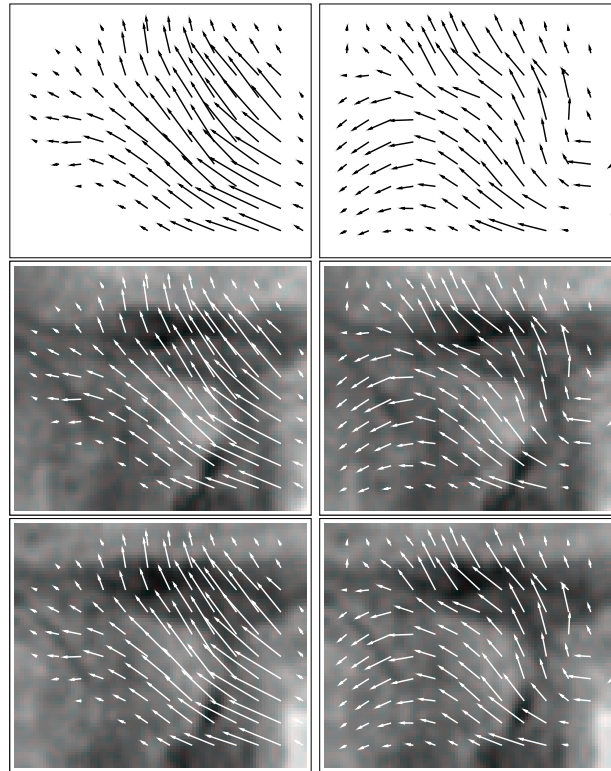


Figure 5. Left: result of IME, Right: result of IMI. Up: motion fields. Center: motion fields superposed to acquisition 3. Bottom: motion fields superposed to acquisition 4.

ANR project Geo-FLUIDS (ANR 09 SYSC 005 02).

REFERENCES

- Béréziat, D. and I. Herlin. Solving ill-posed Image Processing problems using Data Assimilation. *Numerical Algorithms*, 56(2):219–252, February 2011.
- Horn, B. and B. Schunk. Determining optical flow. *Artificial Intelligence*, 17:185–203, 1981.
- Ruhnau, P., A. Stahl, and C. Schnörr. Variational estimation of experimental fluid flows with physics-based spatio-temporal regularization. *Measurement Science and Technology*, 18:755–763, 2007.
- Tarantola, A. *Inverse Problem Theory and Methods for Model Parameter Estimation*. Society for Industrial and Applied Mathematics, 2005.
- Titau, O., A. Vidard, I. Souopgui, and F.-X. L. Dimet. Assimilation of image sequences in numerical models. *Tellus A*, 62:30–47, 2010.
- Tremolet, Y. Accounting for an imperfect model. *Quarterly Journal of the Royal Meteorological Society*, 132(621):483—2504, October 2006.